nature neuroscience

Autism spectrum disorder susceptibility gene *TAOK2* affects basal dendrite formation in the neocortex

Froylan Calderon de Anda[1,2], Ana Lucia Rosario[1,2], Omer Durak[1–3], Tracy Tran[2,4,5], Johannes Gräff[1,2], Konstantinos Meletis[1–3,5], Damien Rei[1,2], Takahiro Soda[1,2], Ram Madabhushi[1,2], David D Ginty[2,4], Alex L Kolodkin[2,4] & Li-Huei Tsai[1–3]

How neurons develop their morphology is an important question in neurobiology. Here we describe a new pathway that specifically affects the formation of basal dendrites and axonal projections in cortical pyramidal neurons. We report that thousand-and-one-amino acid 2 kinase (TAOK2), also known as TAO2, is essential for dendrite morphogenesis. TAOK2 downregulation impairs basal dendrite formation *in vivo* without affecting apical dendrites. Moreover, TAOK2 interacts with Neuropilin 1 (Nrp1), a receptor protein that binds the secreted guidance cue Semaphorin 3A (Sema3A). TAOK2 overexpression restores dendrite formation in cultured cortical neurons from *Nrp1*$^{Sema-}$ mice, which express Nrp1 receptors incapable of binding Sema3A. TAOK2 overexpression also ameliorates the basal dendrite impairment resulting from Nrp1 downregulation *in vivo*. Finally, Sema3A and TAOK2 modulate the formation of basal dendrites through the activation of the c-Jun N-terminal kinase (JNK). These results delineate a pathway whereby Sema3A and Nrp1 transduce signals through TAOK2 and JNK to regulate basal dendrite development in cortical neurons.

Pyramidal neurons are abundant in brain regions associated with complex cognitive functions, including the cortex, hippocampus and amygdala[1]. An understanding of the distinct physiology and morphology of these neurons is key to the elucidation of the mechanisms underlying sophisticated cognitive functions in normal and disease conditions. Several lines of evidence suggest that aberrant dendritic arborization may contribute to neurodevelopmental and psychiatric disorders with delayed onset, such as autism spectrum disorders[2,3]. In general, pyramidal neurons have a dendritic tree that is divided into two domains: the apical dendrite, which extends toward the pial surface, and basal dendrites, which emerge from the base of the cell body. The majority of synapses received by neocortical pyramidal neurons form on the basal dendrites[4]. However, little is known about the molecular pathways that control the formation of basal dendrites.

TAOK1 and TAOK2 serine/threonine protein kinases are known to activate mitogen-activated protein (MAP) kinase (MAPK) pathways (JNK, p38 or extracellular signal-regulated kinase[5,6]), leading to the modulation of gene transcription. In humans, the gene encoding TAOK2, a member of the MAP kinase kinase kinase (MAPKKK) family, is located on chromosome 16p11.2, a region that has recently been shown to carry substantial susceptibility to autism spectrum disorders[7] and schizophrenia[8]. *TAOK2* mRNA is also a direct target of the fragile X protein, FMRP[9], whose loss or dysfunction leads to an autistic phenotype. TAOK2 selectively activates mitogen-activated protein kinases (MEKs)[10] and serves as a regulator of p38 MAPK. In addition, TAOK2 modulates the actin cytoskeleton in non-neuronal cells through the activation of JNK[11]. *TAOK2* is subjected to alternative splicing to produce the TAOK2α (140 kDa) and TAOK2β (120 kDa) isoforms[12], of which only TAOK2α stimulates the JNK pathway[13].

Here we demonstrate that TAOK2 downregulation selectively impairs the formation of basal dendrites and axonal elongation. We found that TAOK2 interacted with Nrp1, the receptor of the secreted guidance cue Sema3A that controls basal dendrite arborization[14–17]. Sema3A induced TAOK2 phosphorylation, thereby activating TAOK2. In conditions in which Nrp1 was either not expressed or was not capable of binding Sema3A, basal dendrite formation deficits could be restored by TAOK2 overexpression. TAOK2 downregulation also led to JNK inactivation that manifested as a decrease of JNK phosphorylation in cultured cortical neurons. Overexpression of a constitutively active JNK1 (MKK7-JNK1) restored basal dendrite formation in cortical neurons after TAOK2 downregulation. Overall, these data support the action of a signaling axis involving Sema3A, Nrp1, TAOK2 and JNK1 in the regulation of basal dendrite formation in the developing cortex.

RESULTS

Expression profile of TAOK2 in neurons and cerebral cortex

To examine the subcellular expression profile of TAOK2, we analyzed TAOK2 immunoreactivity in mouse cortical neurons dissociated at embryonic day (E) 17 and cultured 2 days *in vitro* (DIV). TAOK2 preferentially localized to growth cones (**Fig. 1a**,**b**). The growth cone is a region where actin, but not microtubules, accumulates (**Fig. 1b**)

[1]Department of Brain and Cognitive Sciences, Picower Institute for Learning and Memory, Massachusetts Institute of Technology, Cambridge, Massachusetts, USA. [2]Howard Hughes Medical Institute, Cambridge, Massachusetts, USA. [3]Stanley Center for Psychiatric Research, Broad Institute, Cambridge, Massachusetts, USA. [4]Solomon H. Snyder Department of Neuroscience, The Johns Hopkins University School of Medicine, Baltimore, Maryland, USA. [5]Present addresses: School of Medicine, Rutgers University, Newark, New Jersey, USA. (T.T.) and Department of Neuroscience, Karolinska Institutet, Stockholm, Sweden (K.M.). Correspondence should be addressed to L.-H.T. (lhtsai@mit.edu).

Received 8 March; accepted 14 May; published online 10 June 2012; corrected after print 9 July 2012: doi:10.1038/nn.3141

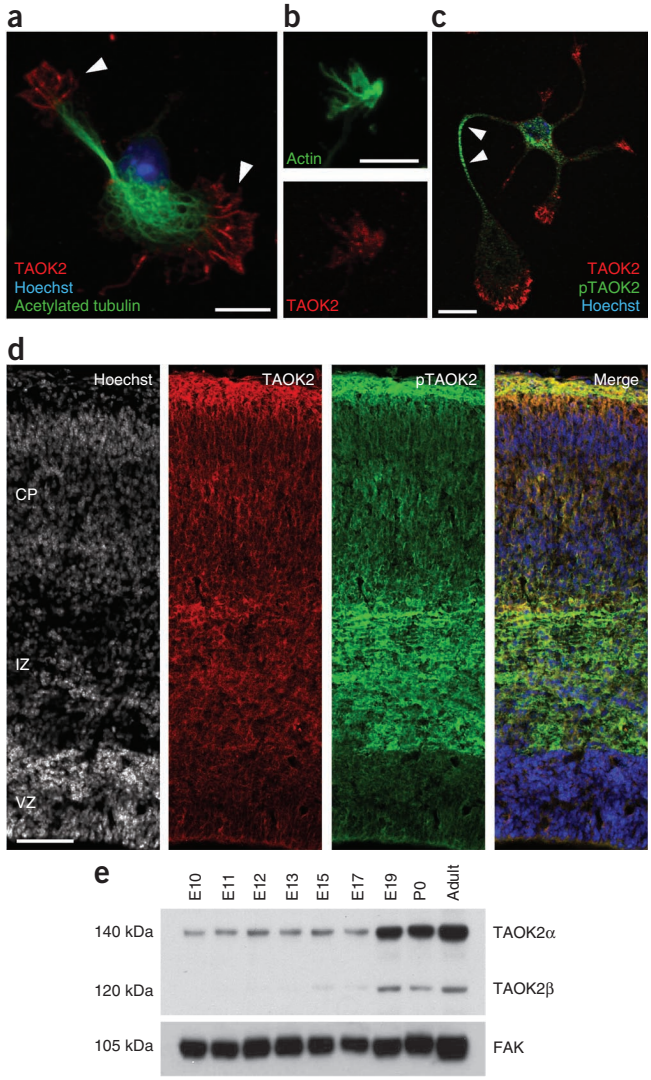

Figure 1 Distribution of TAOK2 and activated TAOK2 in cultured neurons and the developing cerebral cortex. (**a**) TAOK2 localizes to the growth cones (arrowheads) of isolated cortical neurons. (**b**) TAOK2 (red) localizes with actin (green) in growth cones. (**c**) Activated TAOK2 (pTAOK2; green) localizes to the neurite shaft of isolated cortical neurons. (**d**) TAOK2 and pTAOK2 are preferentially present in the intermediate zone (IZ) and cortical plate (CP) of the developing cortex. (**e**) Western blotting. TAOK2α expression is constant during early cortical embryonic development but increases considerably at perinatal (E19, P0) and adult time points. The TAOK2β isoform is absent before E19. Focal adhesion kinase (FAK) is used as a loading control. Scale bars, 10 μm (**a**,**c**), 5 μm (**b**) and 200 μm (**d**); Hoechst stains nuclei.

and where the actin cytoskeleton is the most dynamic[18]. In contrast, TAOK2 activated by phosphorylation on Ser181 (pTAOK2) localized to the neurite shaft, where microtubules also accumulate (**Fig. 1c**). This pattern of TAOK2 expression suggests that TAOK2 may act as a coordinator of actin and microtubule dynamics[19].

In the mouse brain, TAOK2 and pTAOK2 are preferentially expressed in the intermediate zone and the cortical plate of the developing cortex (E18), and their expression in the ventricular zone is low (**Fig. 1d**). Western blot analysis using whole-cell extracts from the cortices of mice at different embryonic and postnatal ages demonstrated that the long isoform of TAOK2 (TAOK2α; 140 kDa) was expressed throughout early cortical embryonic development and increased in perinatal (E19 and postnatal day (P) 0) and adult mice. In contrast, the short isoform of TAOK2 (TAOK2β; 120 kDa) was only observed perinatally and in the adult (**Fig. 1e**). In addition, in DIV2 E17 cortical neurons, we detected expression of TAOK2α but not TAOK2β (data not shown). These results suggest that TAOK2α is likely to be the TAOK2 isoform most important for neuronal differentiation. We therefore focused our subsequent studies on TAOK2α.

TAOK2 affects differentiation in cultured cortical neurons

The remodeling of the actin-based cytoskeleton is an important regulatory step in axon and dendrite formation[20–22]. As it has been shown that TAOK2 modulates the organization of the actin cytoskeleton in non-neuronal cells[11] and we found TAOK2 expression to be concentrated in actin-rich structures, we asked whether TAOK2 loss of function and gain of function affects neuronal differentiation. For this, we designed three specific short hairpin RNAs (shRNAs) targeting different coding sequences of *Taok2* to acutely knock down the expression of TAOK2. We confirmed the specificity of our shRNA constructs with respect to their ability to downregulate endogenous neuronal TAOK2 in cortical neurons at E17 from embryos that had been transfected by *in utero* electroporation at E15 with constructs expressing *Taok2* shRNA or control shRNA and expressing membrane-bound GFP (F-GFP). Neurons were cultured for 48 h before being processed for immunocytochemistry using antibodies to TAOK2 and to acetylated tubulin (**Supplementary Fig. 1a–d**; data not shown for shRNA 3). We also assessed the specificity of our shRNA constructs by western blot analysis in the mouse hippocampal neuronal Ht22 cell line (**Supplementary Fig. 1e,f**; data not shown for shRNA 3). These experiments showed that *Taok2* shRNAs efficiently downregulated TAOK2 expression. We used shRNAs 1 and 2 for all subsequent experiments.

We first examined the impact of TAOK2 knockdown on the cytoskeleton and growth cone morphology in primary neurons. The shRNA-mediated knockdown of TAOK2 decreased the F-actin content in the growth cones of cultured cortical neurons (**Fig. 2a,b**) and the number of intact (non-collapsed) growth cones per neuron, compared with those in control-transfected neurons (**Fig. 2a,c**). In addition, TAOK2 downregulation decreased the number of neurites per neuron (**Fig. 2a,d**) and the number of secondary branches per cell (**Fig. 2a,e**). TAOK2 autophosphorylation is known to activate TAOK2 (refs. 10,13); accordingly, the overexpression of TAOK2 increased phosphorylated, active TAOK2 (**Supplementary Fig. 1g,h**). TAOK2 overexpression in cultured cortical neurons increased the number of primary, but not secondary, neurites compared with those in control neurons (**Fig. 2a,d**).

In addition, we analyzed whether TAOK2 downregulation or overexpression affects polarization in cultured neurons. We found that TAOK2 downregulation impaired axon formation (**Supplementary Fig. 2a**). Of note, TAOK2 overexpression did not affect the number of polarized (axon-bearing) neurons (**Supplementary Fig. 2a**), but it did increase the proportion of neurons that elaborated multiple axons (**Supplementary Fig. 2b,c**). To determine whether these phenotypes resulted specifically from the downregulation of TAOK2, we coexpressed *Taok2* shRNA 1 with a shRNA-resistant version of *TAOK2* cDNA (human *TAOK2* cDNA, *TAOK2*), which rescued the *Taok2* shRNA 1 phenotypes. This molecular replacement experiment further demonstrated the specificity of *Taok2* shRNA 1 treatment (**Fig. 2a–e** and **Supplementary Fig. 2a**). Together, these data demonstrate that TAOK2 is critical for the morphological differentiation of cultured cortical neurons.

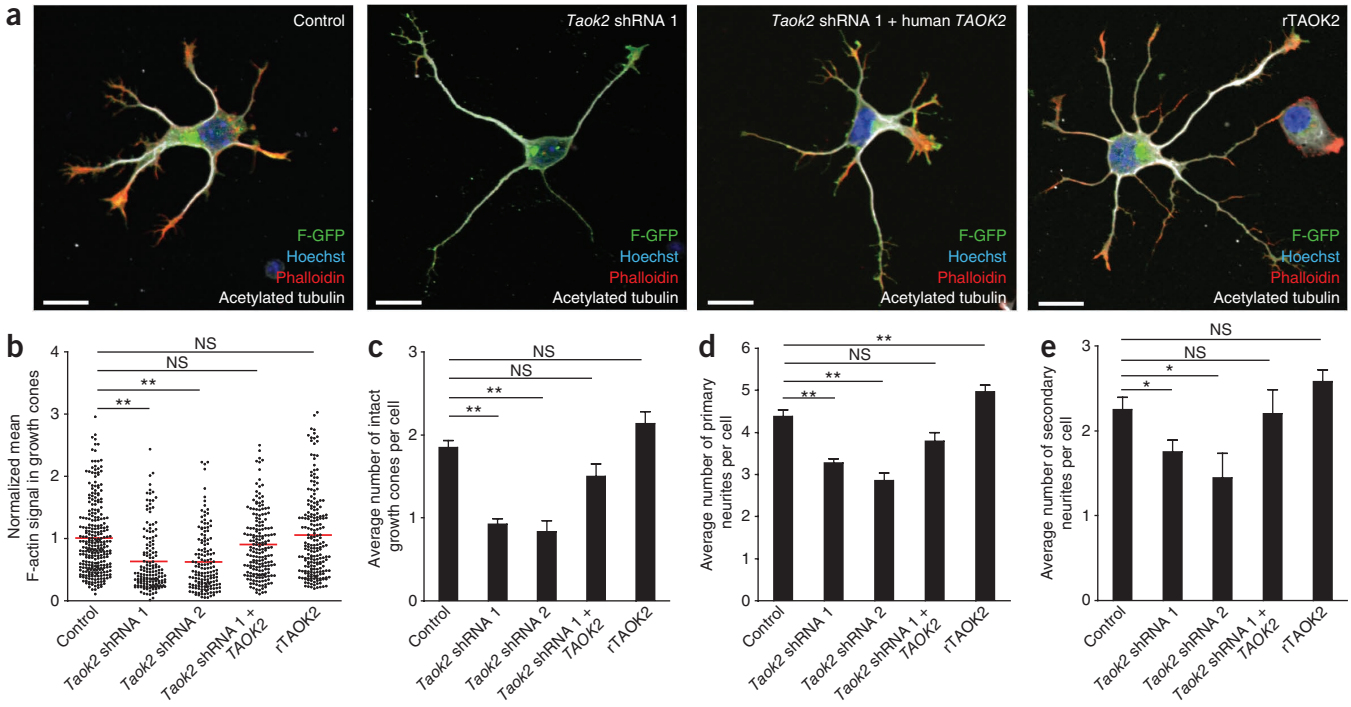

Figure 2 TAOK2 downregulation or overexpression affects the differentiation of isolated cortical neurons. (**a**) TAOK2 downregulation and overexpression have opposite effects on the complexity of cortical neurons. *Taok2* shRNA–transfected neurons show fewer branched neurites and show collapsed growth cones. Expression of an shRNA-resistant human *TAOK2* cDNA counteracts TAOK2 downregulation. rTAOK2 overexpression increases neuronal complexity, with more primary neurites. Phalloidin stains F-actin; Hoechst stains nuclei. (**b**) Quantification of F-actin content in growth cones. TAOK2 silencing decreased F-actin in growth cones (control, $n = 44$ cells, three cultures; *Taok2* shRNA 1, $n = 43$ cells, three cultures; *Taok2* shRNA 2, $n = 36$ cells, two cultures; $P < 0.0001$ by one-way ANOVA, *post hoc* Dunnett test $^{**}P < 0.01$; NS, not significant). (**c**) Number of intact (non-collapsed) growth cones per transfected cell. TAOK2 silencing decreased the number of intact growth cones per cell (control, $n = 160$ cells, three cultures; *Taok2* shRNA 1, $n = 133$ cells, three cultures; *Taok2* shRNA 2, $n = 36$ cells, two cultures; $P < 0.0001$ by one-way ANOVA, *post hoc* Dunnett test $^{**}P < 0.01$). (**d**,**e**) TAOK2 downregulation decreased the number of primary (control, $n = 168$ cells, three cultures; *Taok2* shRNA 1, $n = 149$ cells, three cultures; *Taok2* shRNA 2, $n = 36$ cells, two cultures; $P < 0.0001$ by one-way ANOVA, *post hoc* Dunnett test $^{**}P < 0.01$) and secondary neurites ($P = 0.0102$ by one-way ANOVA, *post hoc* Dunnett test $^{*}P < 0.05$) per transfected cell. rTAOK2 overexpression increased the number of primary neurites (rTAOK2, $n = 119$ cells, three cultures; $P < 0.0001$ by one-way ANOVA, *post hoc* Dunnett test $^{**}P < 0.01$). Mean ± s.e.m. Scale bars, 10 µm.

TAOK2 affects basal dendrite formation and axon elongation

We then sought to determine the effect of TAOK2 on the post-migratory differentiation of cortical neurons *in vivo*. We electroporated E15 mouse embryos *in utero* with *Taok2* shRNA, control shRNA or rat *Taok2* cDNA (*rTaok2*) plasmids together with an F-GFP construct. Mice were killed at P7 and the dendritic morphology of neurons evaluated. Both the knockdown and overexpression of TAOK2 disrupted cortical neuronal differentiation *in vivo*. In layer II-III of the *in utero* electroporated brains, the *Taok2* shRNA–transfected neurons had significantly fewer primary dendrites as compared to controls (**Fig. 3a**,**b**). TAOK2 overexpression, by contrast, increased the number of primary dendrites (**Fig. 3a**,**b**). Sholl analysis of dendritic arbors from shRNA-transfected neurons revealed that TAOK2 downregulation produced less complex basal dendritic arbors than control shRNA transfection. *Taok2* shRNA–transfected neurons had significantly fewer dendritic processes with intersections between 15 µm and 55 µm from the cell soma (**Fig. 3c**). In contrast, TAOK2 overexpression increased the complexity of the dendritic arbor compared to that in control-transfected neurons (**Fig. 3c**). Notably, however, Sholl analysis demonstrated that TAOK2 downregulation or TAOK2 overexpression did not affect the apical dendrites of transfected neurons (**Fig. 3d** and **Supplementary Fig. 3a**).

To determine whether the basal dendrite phenotype was exclusive to upper-layer neurons or was a more general feature of pyramidal neurons in the different cortical layers, we knocked down TAOK2 expression in neurons of a deeper layer (layer V) by *in utero* electroporating E13 embryos with *Taok2* shRNA or control shRNA plasmids together with an F-GFP construct, then evaluated the dendritic morphology of transfected neurons in layer V at P4. TAOK2 downregulation using either shRNA 1 or 2 also impaired the basal dendrite complexity of layer V pyramidal neurons (**Supplementary Fig. 3b**,**c**), without affecting apical dendrite complexity (**Supplementary Fig. 3d**). These findings demonstrate that TAOK2 loss of function or gain of function impairs pyramidal neuron basal dendrite formation in the developing neocortex.

We also examined the contribution of TAOK2 to axon elongation during brain development. We performed sequential *in utero* transfection as previously reported[23]. mCherry fluorescent protein–expressing and control shRNA constructs were introduced into E15 mouse cortex, followed by the introduction of Venus-expressing and *Taok2* shRNA the constructs into the contralateral hemisphere. Callosal axons from transfected neurons crossing into the midline were examined at P7. TAOK2 downregulation impaired axon elongation, and axons were absent in the midline (**Fig. 3e**,**f**). By constrast, TAOK2 overexpression caused some transfected axons to deviate from the axonal tract (**Supplementary Fig. 3e**). These results strongly support action of TAOK2 in axon elongation in the mouse *in vivo*, as was reported in *Drosophila*[19].

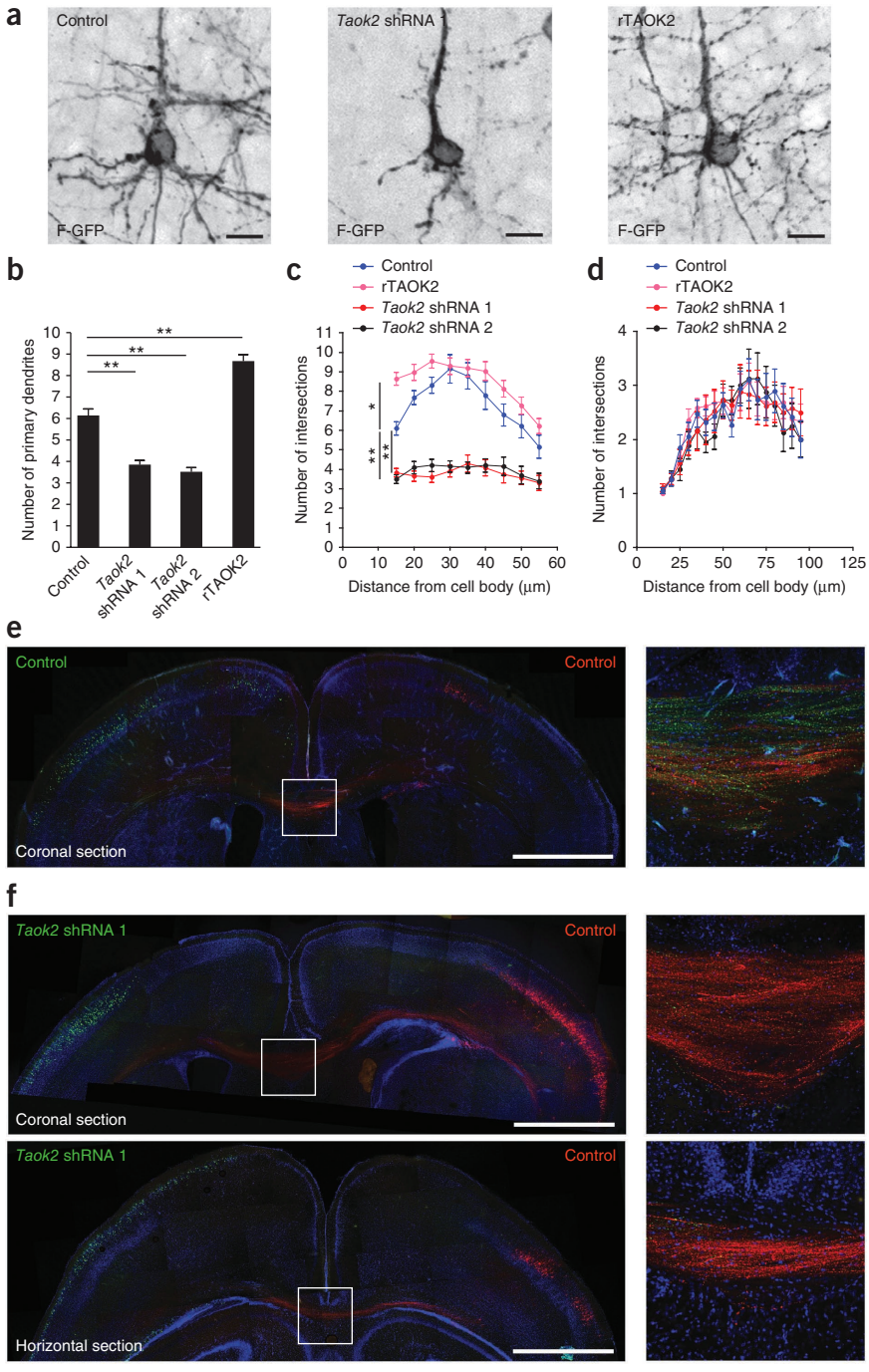

Figure 3 TAOK2 downregulation or overexpression affects basal dendrite arborization and callosal axon projection in the developing cortex. (**a**) TAOK2 knockdown and upregulation had opposite effects in basal dendrite development *in vivo*. (**b**) The number of primary dendrites decreased after TAOK2 knockdown and increases after rTAOK2 overexpression (control, $n = 19$ cells, three brains; *Taok2* shRNA 1, $n = 23$ cells, three brains; *Taok2* shRNA 2, $n = 20$ cells, two brains; rTAOK2, $n = 31$ cells, three brains; $P < 0.0001$ by one-way ANOVA, *post hoc* Dunnett test $^{**}P < 0.01$). (**c**) Sholl analysis of the dendritic arbor from upper cortical layer transfected neurons. $P < 0.0001$ by one-way ANOVA, *post hoc* Dunnett test $^{**}P < 0.01$, $^{*}P < 0.05$. (**d**) Sholl analysis of apical dendrites from cells in **c**. (**e**,**f**) TAOK2 shRNA-mediated downregulation diminished the number of callosal axons traversing the midline ($n = 3$ brains per condition). (**e**) Control transfected neurons in both hemispheres (Venus, left hemisphere; mCherry, right hemisphere) projected callosal axons that crossed the midline. Right panel: corpus callosum inset. (**f**) TAOK2 knockdown in Venus-positive neurons prevented axons from these cells from crossing the midline. Right panels: inset of the corpus callosum outlined in the respective panels at left. Mean ± s.e.m. Scale bars, 10 μm (**a**) and 500 μm (**e**,**f**).

TAOK2 interacts with Neuropilin 1 to modulate differentiation

Previous studies have shown that the Sema3A–Nrp1/PlexinA4 signaling cascade controls basal dendritic arborization[14–16]. *Nrp1*$^{Sema-}$ mice also develop axonal projection defects in the corpus callosum and the hippocampus[14]. These defects vary from mild phenotypes, in which some axons deviate from the axonal tract, to more severe ones, in which callosal axons defasciculate and do not cross the midline[14]. We hypothesized that TAOK2 may interact with this pathway to modulate neuronal differentiation. To test this idea, we performed coimmunoprecipitation experiments to probe for an interaction between TAOK2 and Nrp1. We coexpressed TAOK2 and Nrp1-mCherry in HEK-293T human embryonic kidney cells and found that TAOK2 interacted with Nrp1-mCherry (**Fig. 4a**). To investigate whether this complex also forms *in vivo*, cortices from P0 mice were homogenized and subjected to coimmunoprecipitation using antibodies to Nrp1 and TAOK2. Nrp1 associated with TAOK2 in lysates from P0 mouse cortices (**Fig. 4b**).

TAOK2 is activated by phosphorylation on Ser181, which resides in the activation loop of the kinase[24]. To determine whether Sema3A/Nrp1 activates TAOK2, we first examined whether active TAOK2 colocalizes with Nrp1. In the mouse E19 cerebral wall, we found that pTAOK2 and Nrp1 colocalized preferentially in the intermediate zone and lower cortical plate, where axons elongate and deeper layer neurons begin to form dendrites[25] (**Fig. 4c**,**d**).

Next, we examined whether the Nrp1 ligand Sema3A modulates TAOK2 phosphorylation in cultured primary neurons. Cortical neurons dissociated from E17 mouse embryos and cultured for 48 h were treated with Sema3A (2 μg ml^{-1}) for 30 min, 1 h, 2 h, or 6 h. pTAOK2 immunoreactivity after Sema3A treatment increased significantly between 1 and 6 h in the longest neurite analyzed (the putative axon, neurite length between 40 and 150 μm) as compared to that in untreated control cells (**Fig. 4e**,**f**). Western blot analysis of lysates from neurons after 2 h of Sema3A treatment revealed that endogenous TAOK2 phosphorylation was also induced after Sema3A treatment (**Fig. 4g**; normalized to control: control, 1 ± 0.03-fold; Sema3A, 1.32 ± 0.14-fold increase versus control; $n = 3$ experiments per duplicate; $P = 0.0401$ by t test). Finally, we quantified pTAOK2 in cortical extracts from mice homozygous for a knock-in mutation that renders

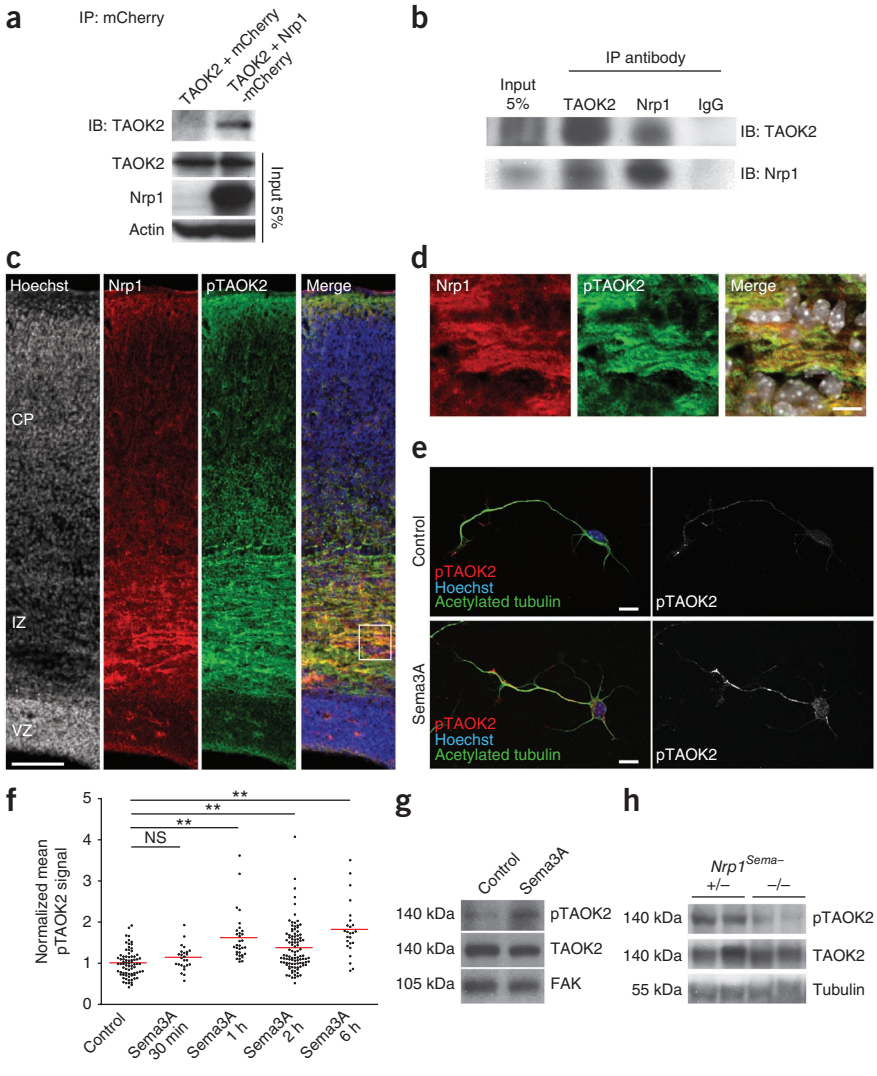

Figure 4 TAOK2 interacts with Nrp1 to modulate TAOK2 phosphorylation. (**a**) Immunoprecipitation (IP) with anti-mCherry demonstrating the interaction of Nrp1 and TAOK2. HEK-293T cells were transfected with Nrp1-mCherry and Myc-TAOK2. Input, 5% of the total protein used for immunoprecipitation. IB, immunoblot. (**b**) TAOK2 coimmunoprecipitates with Nrp1 in the developing cortex. Input, 5% of the total protein used for immunoprecipitation; IgG, immunoglobulin G. (**c**) Nrp1 and pTAOK2 are preferentially expressed in the intermediate zone (IZ) and cortical plate (CP) of the developing cortex. (**d**) Magnification of white box in **c**: Nrp1 and pTAOK2 co-localize in the developing cortex. (**e**–**g**) Sema3A treatment (2 μg ml^{-1}) increases pTAOK2 immunoreactivity in cultured cortical neurons. (**e**) Control neuron (top) and a neuron treated with Sema3A for 2 h (bottom). (**f**) Quantification of pTAOK2 immunoreactivity from the longest neurite of control and Sema3A-treated cultured cortical neurons (control, $n = 77$ cells, three cultures; Sema3A 30 min, $n = 25$ cells, two cultures; Sema3A 1 h, $n = 32$ cells, three cultures; Sema3A 2 h, $n = 99$ cells, three cultures; Sema3A 6 h, $n = 25$ cells, three cultures; $P < 0.0001$ by one-way ANOVA, *post hoc* Dunnett test $^{**}P < 0.01$ and NS, not significant). (**g**) Immunoblot of cultured cortical neuron lysates showing that the 2-h Sema3A treatment increases pTAOK2 immunoreactivity. (**h**) Immunoblot of cortical lysates from *Nrp1*$^{Sema-}$ heterozygous (+/–) and *Nrp1*$^{Sema-}$ homozygous (–/–) P7 mice littermates showing less pTAOK2 immunoreactivity in the –/– mouse than in the +/– littermate. FAK and tubulin are used as loading controls. Scale bars, 500 μm (**c**) and 10 μm (**d**,**e**).

the endogenous Nrp1 receptor incapable of binding Sema3A (*Nrp1*$^{Sema-}$). In agreement with our *in vitro* experiments, we found that pTAOK2 amounts were lower in the cortical neurons of homozygous *Nrp1*$^{Sema-}$ (–/–) mice than in those of heterozygous (+/–) littermates (**Fig. 4h**; normalized to +/–: for +/–, 1 ± 0.10, $n = 9$ brains; for –/–, 0.56 ± 0.09, $n = 4$ brains; $P = 0.0310$ by t test). These results suggest that Sema3A signaling activates TAOK2 kinase activity.

TAOK2 and Sema3A modulate JNK activity in cortical neurons

We next sought to elucidate the downstream effectors by which the interaction of TAOK2 with the Sema3A-Nrp1 signaling pathway modulates neuronal differentiation in cortical pyramidal neurons. The JNKs have been shown to be important for many aspects of neuronal differentiation[26]. TAOK2α, unlike TAOK2β, stimulates the JNK pathway in cell lines[13]. TAOK2 overexpression indirectly activates endogenous JNK1 in HEK-293T cells through the preferential phosphorylation of MEK3 and MEK6 (ref. 5). In addition, TAOK2 has been shown to modulate the dual phosphorylation of JNK1 at Thr183 and Tyr185 (refs. 5,27). Sema3A has also been shown to activate the JNK1–c-Jun signaling pathway in cultured dorsal root ganglion neurons[28]. Phosphorylated JNK1 and 2 can modulate neurite initiation, axon formation and dendritic architecture in cultured neurons[29–33] and is required for the maintenance of neuronal microtubules in axons and dendrites *in vivo*[34]. The deactivation of JNK1 by BDNF treatment destabilizes microtubules and induces axonal branching[35]. On the basis of these findings, we hypothesized that JNK1 may mediate the effect of TAOK2 and Sema3A on neuronal differentiation.

To determine whether TAOK2 modulates JNK1 in cortical neurons, we introduced *Taok2* shRNA 1 construct or control plasmids together with an F-GFP construct into E15 mouse embryos via *in utero* electroporation and isolated cortical neurons at E17. These neurons were cultured for 48 h before being subjected to immunocytochemistry using antibodies to phosphorylated JNK1 (pJNK; Thr183 and Tyr185), which represents the active form of JNK1. TAOK2 downregulation decreased pJNK1 immunoreactivity in the longest neurite of shRNA-transfected neurons, compared to that of control-transfected neurons (**Fig. 5a**,**b**). Additionally, in Ht22 cells transfected with *Taok2* shRNA 1, endogenous pJNK1 (top panel, lower band, 46 kDa) was significantly reduced (**Fig. 5c**; normalized to control: control, 1 ± 0.17; *Taok2* shRNA 1, 0.76 ± 0.09, $n = 4$ experiments per triplicate; $P = 0.0233$ by t test).

As TAOK2 interacts with Nrp1, we asked whether treatment with the Nrp1 ligand Sema3A modulates JNK1 phosphorylation in cultured primary neurons. Since JNK1 phosphorylation is enriched in developed axons[31], we used cultured neurons during the initiation of polarization to avoid endogenous JNK1 phosphorylation, which could mask that induced by our Sema3A treatment. Cortical neurons dissociated from E17 mouse embryos and cultured for 48 h were

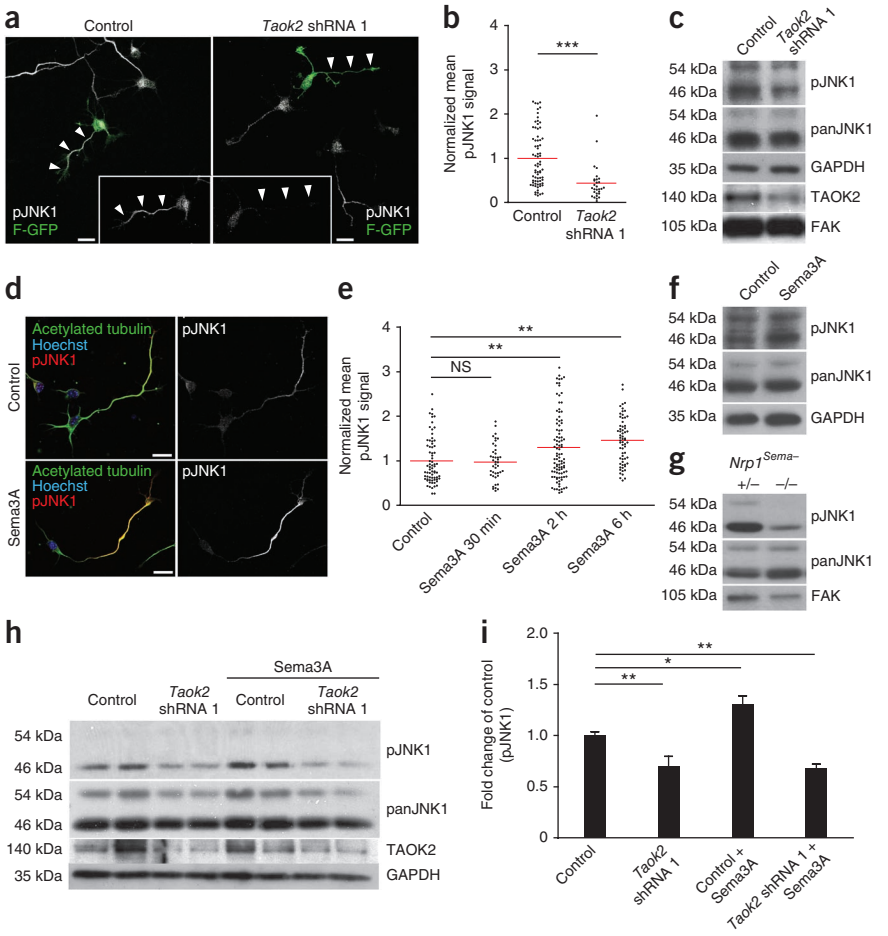

Figure 5 TAOK2 and Sema3A modulate the activity of JNK1. (**a**) TAOK2 downregulation (right) decreases pJNK1 immunoreactivity (arrowheads) in cortical neurons compared to that in control neurons (left). Inset: pJNK1 signal in transfected neurons. (**b**) Quantification of pJNK1 immunoreactivity in the longest neurite of control and TAOK2-downregulated cortical neurons (control, $n = 72$ cells, two cultures; *Taok2* shRNA 1, $n = 29$ cells, two cultures; $^{***}P < 0.0001$ by t test). (**c**) TAOK2 downregulation decreases JNK1 phosphorylation (46 kDa) in Ht22 cells. (**d**–**f**) Sema3A treatment (2 μg ml^{-1}) increases pJNK1 immunoreactivity in cortical neurons. (**d**) Control neuron (top) and a neuron treated with Sema3A for 2 h (bottom). (**e**) Quantification of pJNK1 immunoreactivity from the longest neurite of control and Sema3A-treated cortical neurons (control, $n = 71$ cells, three cultures; Sema3A 30 min, $n = 42$ cells, two cultures; Sema3A 2 h, $n = 97$ cells, three cultures; Sema3A 6 h, $n = 64$ cells, three cultures; $P < 0.0001$ by one-way ANOVA, *post hoc* Dunnett test $^{**}P < 0.01$ and NS, not significant). (**f**) Immunoblot of cultured cortical neuron lysates shows that Sema3A 6h treatment increases pJNK1 immunoreactivity (46 kDa) compared to control. (**g**) Immunoblot of cortex lysates from *Nrp1*$^{Sema-}$ +/– and –/– P7 littermate mice shows less pJNK1 immunoreactivity (46 kDa) in the –/– mouse than in the +/– littermate. (**h**) Western blotting showing that isolated cortical neurons infected with *Taok2* shRNA 1 lentivirus failed to increase pJNK1 in the presence of Sema3A 6 h. (**i**) Quantification of pJNK1 (46 kDa) immunoreactivity from **h** ($n = 2$ experiments per triplicate; $P < 0.0001$ by one-way ANOVA, *post hoc* Dunnett test $^{**}P < 0.01$, $^{*}P < 0.05$). FAK and glyceraldehyde 3-phosphate dehydrogenase (GAPDH) are used as the loading controls; panJNK1, antibody labeling total JNK1. Mean ± s.e.m. Scale bars, 10 μm.

treated with Sema3A (2 μg ml^{-1}) for 30 min, 2 h, or 6 h. The levels of pJNK1 were measured using immunocytochemistry and western blot analysis. pJNK1 immunoreactivity was significantly increased at 2 h and 6 h following Sema3A treatment in the longest neurite analyzed (the putative axon, 40 μm < neurite length < 150 μm) compared to that in non-treated control cells (**Fig. 5d**,**e**). Western blot analysis of lysates harvested from neurons following 6 h of Sema3A treatment revealed that endogenous JNK1 phosphorylation (pJNK, top panel, lower band, 46 kDa) was also induced following Sema3A treatment (**Fig. 5f**; normalized to control: control = 1 ± 0.06, Sema3A = 1.59 ± 0.19; $n = 3$ experiments per duplicate; $P = 0.0014$ by t test). We also examined the levels of pJNK1 in cortical extracts from *Nrp1*$^{Sema-}$ mice. In agreement with our *in vitro* experiments, we found that pJNK1 levels were reduced in the cortical neurons of homozygous *Nrp1*$^{Sema-}$ mice compared with those in heterozygous littermates (**Fig. 5g**; normalized to +/–: for +/–, 1 ± 0.11, $n = 9$ brains; for –/–, 0.54 ± 0.13, $n = 4$ brains; $P = 0.0382$ by t test).

Sema3A and TAOK2 may modulate JNK1 by means of a common mechanism; alternatively, they may regulate JNK1 by means of distinct pathways. To differentiate between these possibilities, we evaluated JNK1 activation after Sema3A treatment in the absence or presence of TAOK2. Primary neurons were infected with recombinant lentivirus carrying control or *Taok2* shRNA 1 soon after plating. Three days later, we quantified pJNK1 after the addition of exogenous Sema3A (2 μg ml^{-1}). Sema3A increased pJNK1 in control shRNA-treated neurons by about 30–40% (**Fig. 5h**,**i**). Notably, Sema3A did not elevate pJNK1 when TAOK2 was knocked down (**Fig. 5h**,**i**). These results indicate that TAOK2 is required for Sema3A to induce pJNK1. Together, these data suggest that the interaction of TAOK2 with the Sema3A-Nrp1 signaling complex activates JNK1 phosphorylation to mediate neuronal differentiation in cortical pyramidal neurons.

Sema3A-Nrp1 modulates basal dendrite formation through TAOK2

Little is known about the molecular pathways that determine the formation of basal dendrites in pyramidal neurons. Therefore, we decided to analyze whether TAOK2 modulates basal dendrite formation downstream of Sema3A-Nrp1. To this end, we examined whether TAOK2 overexpression is sufficient to restore the defect in dendrite arborization observed in neurons from *Nrp1*$^{Sema-}$ mice[14,15]. These mice exhibit markedly reduced branching and growth of basal dendrites in layer V cortical neurons[14,15]. In contrast, wild-type neurons *in situ* treated with Sema3A increase their dendritic complexity[17]. We overexpressed TAOK2 in neurons dissociated from the E13.5 cortex of *Nrp1*$^{Sema-}$ and wild-type mice. At DIV7, Sema3A treatment of *Nrp1*$^{Sema-}$ neurons did not restore the reduced dendritic arborization complexity to wild-type levels, confirming the inability of the *Nrp1*$^{Sema-}$ receptor to bind Sema3A (**Fig. 6a**,**b**). However, TAOK2

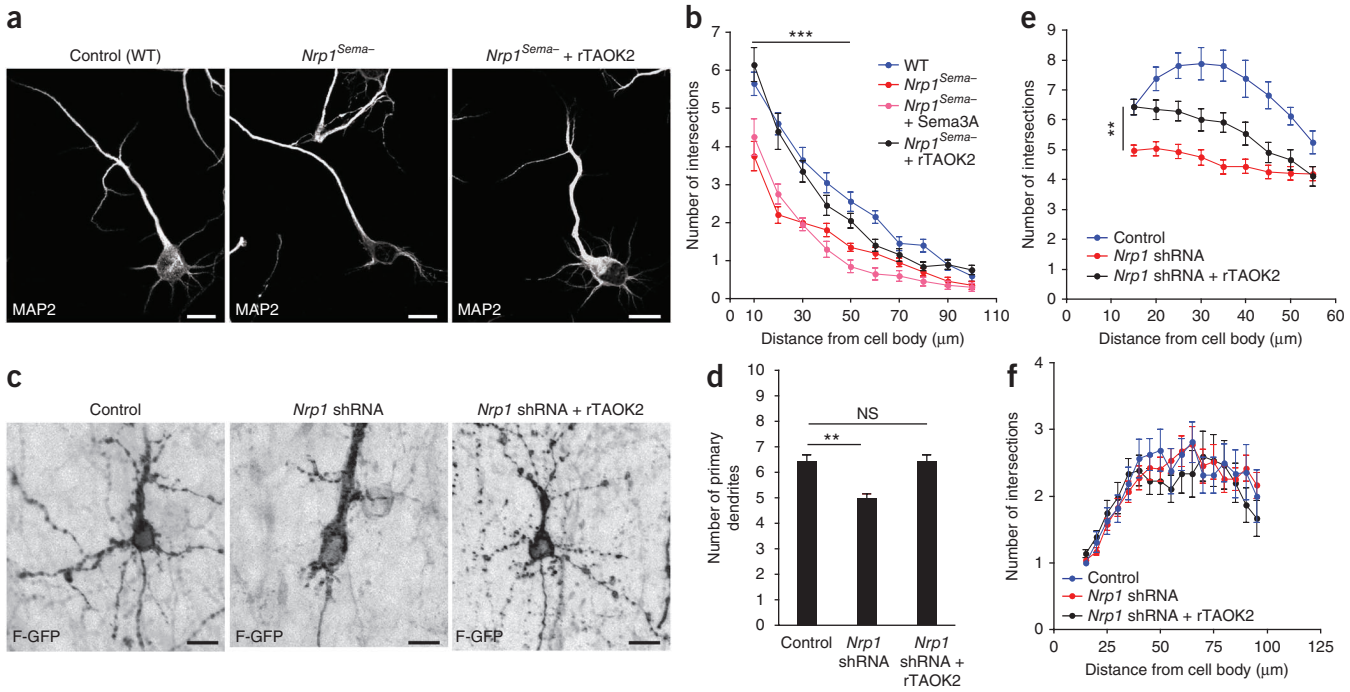

Figure 6 TAOK2 counteracts the dendritic arborization deficit in neurons expressing a deficient receptor for Nrp1 or with Nrp1 downregulation. (**a**) rTAOK2 overexpression ameliorates the dendritic arborization deficit in primary cortical *Nrp1*$^{Sema-}$ neurons. (**b**) Sholl analysis of the dendritic arbors, showing no statistical differences between wild-type (WT) neurons and *Nrp1*$^{Sema-}$ plus rTAOK2-overexpressing cultured neurons at a distance between 10 μm and 100 μm from the cell soma ($n = 20$ cells per condition, two cultures, $^{***}P < 0.001$ by t test). (**c**) rTAOK2 overexpression reverses the basal dendritic arborization deficit in *Nrp1* shRNA-transfected neurons from layer II-III cortex. (**d**) rTAOK2 overexpression restores the number of primary dendrites in Nrp1 downregulated neurons (control, $n = 16$ cells, two brains; *Nrp1* shRNA, $n = 47$ cells, three brains; *Nrp1* shRNA plus rTAOK2, $n = 35$ cells, three brains; $P < 0.0001$, by one-way ANOVA, *post hoc* Dunnett test $^{**}P < 0.01$ and NS, not significant). (**e**) Sholl analysis of the dendritic arbors, showing significant differences between *Nrp1* shRNA–expressing neurons and Nrp1 shRNA + rTAOK2–expressing neurons ($P < 0.0001$ by one-way ANOVA, *post hoc* Dunnett test $^{**}P < 0.01$). (**f**) Sholl analysis of the apical dendrite, showing no differences between Nrp1 downregulation, *Nrp1* shRNA + rTAOK2 overexpression, and control conditions. Mean ± s.e.m. Scale bars, 10 μm.

overexpression ameliorated the defective dendritic arborization in *Nrp1*$^{Sema-}$ neurons (**Fig. 6a**,**b**). Sholl analysis of the dendritic arbors located between 10 μm and 100 μm from the cell soma showed that dendritic arborization was restored to wild-type levels in the *Nrp1*$^{Sema-}$ TAOK2-overexpressing neurons (**Fig. 6b**).

To further confirm the functional interaction of TAOK2 and Nrp1 *in vivo*, we acutely knocked down the expression of Nrp1 using an shRNA construct and overexpressed TAOK2 simultaneously in layer II-III cortical neurons by *in utero* electroporation. The *Nrp1* shRNA sequence was previously reported to downregulate Nrp1 expression in the cortex[16], and we confirmed that it efficiently knocked down the expression of Nrp1-mCherry in HEK-293T cells (**Supplementary Fig. 4a**,**b**). E15 embryos were *in utero* electroporated with the *Nrp1* shRNA plasmid or a control shRNA plasmid, together with *F-GFP* and *rTaok2* cDNA constructs, and studied at P7. We evaluated the dendritic morphology in neurons of the layer II-III cortex from control and *Nrp1* shRNA–expressing brains. The knockdown of Nrp1 impaired the formation of basal dendrites in the upper cortical layers (II-III; **Fig. 6c**), as has been previously reported[16]. Notably, TAOK2 overexpression ameliorated the basal dendrite arborization deficit in *Nrp1* shRNA-expressing neurons (**Fig. 6c**). TAOK2-overexpressing neurons showed a significantly increased primary basal dendrite number in neurons with Nrp1 knockdown; this number was not significantly different from that of controls (**Fig. 6d**). However, using Sholl analysis, we found that the basal dendritic branching (secondary branching) was not restored to control levels (**Fig. 6e**). Sholl analysis also demonstrated that Nrp1 downregulation did not affect the apical dendrites of transfected neurons (**Fig. 6f**). These results reflect a partial restoration of the formation of basal dendrites following TAOK2 expression in Nrp1-deficient neurons. Our results thus provide evidence that Nrp1 and TAOK2 constitute a pathway that regulates basal dendrite development in pyramidal neurons of the developing cortex.

TAOK2 modulates basal dendrite formation through JNK

Activated JNK1 has been shown to preferentially localize to the longest neurite, presumably the axon, of cultured hippocampal neurons[31]. However, pJNK1 has also been reported to be involved in the regulation of microtubule dynamics in axons, as well as dendrites, in both hippocampus and cortex[34]. Furthermore, JNK1-deficient mice exhibit a progressive loss of microtubules in both axons and dendrites[34]. Until now, it has remained unclear whether pJNK1 modulates microtubules in basal or apical dendrites.

To assess the localization of pJNK1 in cortical pyramidal neurons, we examined its subcellular localization in DIV7 mouse cortical neurons dissociated at E17. We analyzed cells that displayed a pyramidal morphology bearing a thick 'apical' dendrite and several thin 'basal' dendrites. We observed that pJNK1 was enriched in developed axons (**Fig. 7a**) as previously reported[31]. Of note, we also found that the basal dendrites showed a significant increase in the intensity of pJNK1 immunoreactivity, normalized to tubulin or MAP2 immunoreactivity, compared with that in the apical dendrite (**Fig. 7a–c**). Thus, the compartmentalization of pJNK1 might function in the preferential elongation of basal versus apical dendrites.

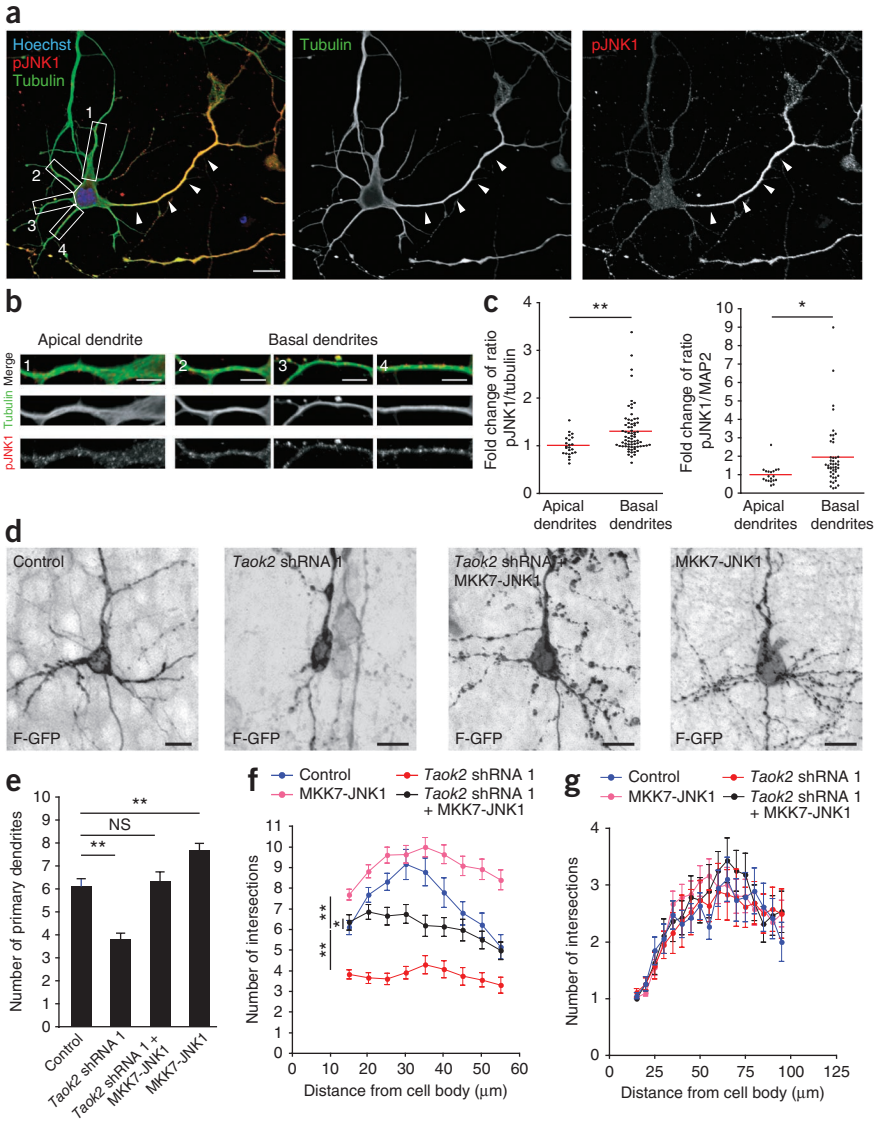

Figure 7 Activated JNK1 ameliorates deficient basal dendrite formation after TAOK2 downregulation. (**a**) Cultured cortical pyramidal neuron immunolabeled for tubulin (green) and pJNK1 (red). Activated JNK1 is enriched in the axon (arrowheads). (**b**) The apical dendrite (1) and basal dendrites (2, 3, 4) outlined in **a**. (**c**) Ratio of pJNK1 and tubulin or MAP2 fluorescence intensities, showing higher ratios of pJNK1 to tubulin and pJNK1 to MAP2 in basal dendrites than in apical dendrites. Values are normalized to the mean of apical dendrites (tubulin, $n = 23$ cells, three cultures; MAP2, $n = 20$ cells, three cultures; $^{**}P = 0.0051$, $^{*}P = 0.0154$ by t test). (**d**) Upper cortical layer (II-III) transfected neurons, showing underdeveloped basal dendrites after shRNA-mediated knockdown of TAOK2 compared with control-transfected neurons. MKK7-JNK1 overexpression ameliorates the basal dendrite deficit following *Taok2* shRNA–mediated downregulation. MKK7-JNK1 overexpression alone increases the number of basal dendrites compared with that in control-transfected cells. (**e**) The number of primary dendrites increases after MKK7-JNK1 overexpression (control, $n = 19$ cells, three brains; *Taok2* shRNA 1, $n = 23$ cells, three brains; *Taok2* shRNA 1 + MKK7-JNK1, $n = 32$ cells, three brains; MKK7-JNK1, $n = 42$ cells, three brains; $^{***}P < 0.0001$ by one-way ANOVA, *post hoc* Dunnett test $^{**}P < 0.01$ and NS, not significant). (**f**) Sholl analysis of the dendritic arbor from upper cortical layer transfected neurons ($^{***}P < 0.0001$ by one-way ANOVA, *post hoc* Dunnett test $^{**}P < 0.01$, $^{*}P < 0.05$). (**g**) Sholl analysis of apical dendrites from cells in **f**. Quantifications for control and *Taok2* shRNA 1–transfected cells are the same as in **Figure 3b–d**. Mean ± s.e.m. Scale bars, 10 μm (**a**,**d**) and 5 μm (**b**).

To further investigate the relationship between TAOK2 and JNK1 in basal dendritic arborization, we determined whether the addition of pJNK1 was able to abrogate the basal dendrite phenotypes caused by TAOK2 loss of function. It had previously been shown that fusing MKK7 to JNK1 (MKK7-JNK1) renders JNK1 constitutively active, thus mimicking the activity of pJNK1 (refs. 36,37). We electroporated E15 mouse embryos *in utero* with *Taok2* shRNA 1 or control shRNA together with F-GFP and MKK7-JNK1 cDNA constructs, and analyzed them at P7. TAOK2 downregulation impaired the formation of primary dendrites in layer II-III neurons (**Fig. 7d**,**e**). Notably, the number of primary dendrites of transfected neurons was markedly increased when MKK7-JNK1 was expressed alone or with *Taok2* shRNA 1 (**Fig. 7d**,**e**). Sholl analysis demonstrated significant differences in the dendritic arborization between neurons expressing *Taok2* shRNA 1, neurons expressing *Taok2* shRNA 1 + MKK7-JNK1 and neurons expressing MKK7-JNK1 at a distance between 15 μm and 55 μm from the cell soma (**Fig. 7f**). However, neurons expressing *Taok2* shRNA and MKK7-JNK1 produced basal dendrites that were not as elaborated as those produced from control shRNA–transfected neurons (**Fig. 7f**). This result reflects a partial restoration of the branching of basal dendrites in *Taok2* shRNA–transfected neurons after the expression of MKK7-JNK1. Notably, MKK7-JNK1 overexpression with or without TAOK2 downregulation did not affect apical dendrite morphology as compared with that of control-transfected neurons (**Fig. 7g**), further supporting a preferential basal dendrite compartmentalization of pJNK. We also found that the active JNK1 rescued the callosal axon deficit in the midline after TAOK2 downregulation (**Supplementary Fig. 5**). Together, these experiments provide evidence that TAOK2 and JNK1 modulate neuronal differentiation in cortical pyramidal neurons, and collectively, these results delineate a molecular pathway whereby TAOK2 governs the morphogenesis of pyramidal neurons in the developing cortex.

DISCUSSION

Here we describe a new molecular pathway that preferentially modulates the formation of basal dendrites in cortical pyramidal neurons and that also functions in axonal projection. Extensive work has addressed the actions of several molecules in dendrite arborization (for review, see ref. 38). However, little is known about the molecular differences that may direct the formation of different domains within the same dendritic tree. Our work aimed to understand the mechanisms responsible for the delineation of basal and apical dendrites during pyramidal neuron development in the embryonic cortex.

Over a decade ago, electron microscopy studies in cultured neurons indicated that axons contain microtubules of uniform polarity, whereas dendrites contain microtubules of mixed polarity[39]. These data support the concept of the molecular homogeneity of the dendritic tree. However, it was recently found that apical dendrites from hippocampal CA1 and cortical layer V pyramidal neurons ubiquitously have polarized microtubule arrays[40], suggesting that the morphogenesis of dendritic subtypes (for example, basal versus apical dendrites) may rely upon distinct cellular and molecular pathways. Accordingly, it was shown that post-Golgi membrane trafficking is polarized toward the apical dendrites of pyramidal neurons and that the disruption of Golgi polarity produces neurons with symmetric dendritic arbors, which lack a single longest principal, or apical, dendrite[41].

The Sema3A-Nrp1 signaling cascade is coupled to TAOK2-JNK1

In previous reports, activation of the Nrp1 receptor by Sema3A appeared to regulate neuronal polarization[42,43]. It was also shown that Sema3A–Nrp1 signaling through PlexinA4 controls the basal dendritic arborization of cortical neurons[14–16]. As the Nrp1 receptor is likely to be uniformly distributed on all dendritic processes[15], as well as the axon[44], one question that arises is how this ubiquitous receptor specifically controls the formation of basal dendrites.

We now show that TAOK2 downregulation specifically impairs the formation of basal dendrites, without affecting apical dendrites. These data strongly suggest that TAOK2 is a mediator of the Sema3A–Nrp1 pathway that sustains basal dendrite formation. Our biochemical analyses demonstrate that TAOK2 and Nrp1 form a complex, and that acute Nrp1 downregulation specifically impairs the formation of the basal dendrite. Importantly, we report that the deficit in basal dendrite formation following Nrp1 downregulation can be counteracted by TAOK2 overexpression.

Our data also show that TAOK2 appears to be uniformly distributed in the growth cones of cultured developing cortical neurons, without any preference for dendritic or axonal neurites. It is possible that our methods could not detect a differential subcellular distribution of TAOK2. Alternatively, the subcellular compartmentalization of molecules that sustain basal dendrite formation may occur downstream of TAOK2.

This work implicates activated JNK1 as an effector of TAOK2 that modulates basal dendrite morphogenesis. It has been shown that pJNK1 is enriched in axons of hippocampal neurons in culture[31]. We also found that pJNK1 was preferentially localized to the longest neurite, presumably the axon, of DIV2 cultured cortical neurons. It has also been reported that pJNK1 is involved in the regulation of microtubule dynamics in both axons and dendrites of the hippocampus and cortex[34] and that JNK1$^{-/-}$ mice exhibit a progressive loss of microtubules in both axons and dendrites[34]. However, the function of pJNK in the different domains of the dendritic tree has not been clear. *In vivo* experiments examining the loss of function of the MAP kinase phosphatase 1 (MKP-1), which deactivates JNK1, show reduced dendritic arborization of cortical pyramidal neurons, as well as impaired axonal branching[35]. In agreement with these findings, we found that pJNK1 was preferentially enriched in the basal dendrites and the axons of cortical pyramidal neurons. Moreover, overexpression of the constitutively active JNK1 counteracted defects in basal dendrite formation and axonal projection after TAOK2 downregulation. Therefore, it is plausible that the subcellular compartmentalization of pJNK1 may explain, at least in part, the specific action of TAOK2 in basal dendrite formation and axonal projection (**Supplementary Fig. 6**). Our results demonstrate that Sema3A/Nrp1-mediated activation of pJNK1 requires TAOK2 (**Fig. 5h,i**), which indicates that the three proteins act in the same pathway. Although additional independent pathways could activate JNK, the existence of such pathways does not preclude the importance of the observed TAOK2-mediated activation of JNK1 in regulating dendrite morphogenesis.

TAOK2 and autism spectrum disorders

Autism spectrum disorder (ASD) is a heterogeneous neurodevelopmental syndrome for which there is not a clear neurobiological etiology. Although the genetic underpinnings of ASD remain elusive in most cases, a unifying model for ASD has recently been suggested[45]. This model proposes that ASD results from a developmental disconnection of brain regions that are involved in higher-order associations. Emerging literature, which shows functional and anatomical cortical hypoconnectivity in autistic patients, supports this model[45,46]. The cellular basis for dysfunctional circuits, however, remains poorly understood.

Several genes have been described as contributing to ASD[47–49], and it has been proposed that aberrant synaptic protein synthesis may represent one pathway leading to an autistic phenotype[50]. Recently, a recurrent microdeletion or reciprocal microduplication of chromosome 16p11.2 has been identified that carries substantial susceptibility to autism and appears to account for approximately 1% of cases[7]. One of the genes from the affected region encodes for TAOK2. Therefore, our findings of immature basal dendrite development and axonal projections deficits following TAOK2 downregulation support the hypothesis that underdeveloped neuron morphology contributes to the disconnection of brain regions that may underlie the autistic phenotype.

METHODS

Methods and any associated references are available in the online version of the paper.

Note: Supplementary information is available in the online version of the paper.

ACKNOWLEDGMENTS

We thank A. Mungenast, E.J. Kwon, M.H. Cobb (University of Texas Southwestern Medical Center) and Y. Gotoh (University of Tokyo) for critical reading of the manuscript, providing vectors, antibodies, and suggestions. The Simons Foundation Autism Research Initiative supported this work. F.C.d.A. is supported by a postdoctoral fellowship from the Simons Foundation (Simons Center for the Social Brain, Massachusetts Institute of Technology). US National Institutes of Health grant R01 MH59199 to A.L.K. and D.D.G. supported this work. L.-H.T., A.L.K. and D.D.G. are investigators of the Howard Hughes Medical Institute.

AUTHOR CONTRIBUTIONS

This study was designed, directed and coordinated by F.C.d.A. and L.-H.T. L.-H.T., as the principal investigator, provided conceptual and technical guidance for all aspects of the project. F.C.d.A. planned and performed the *in utero* electroporations and analyzed the data with A.L.R. and O.D. F.C.d.A. performed and analyzed the immunohistochemistry experiments. K.M. generated and characterized the shRNA constructs. K.M., A.L.R. and D.R. contributed to the neuronal cultures. T.T. performed and analyzed the data from the neuronal cultures of *Nrp1*$^{Sema-}$ mice. A.L.R., O.D., J.G. and R.M. contributed to the biochemistry experiments. T.S. generated the lentiviral shRNA construct and produced the virus particles. D.D.G. and A.L.K. provided the *Nrp1*$^{Sema-}$ mouse brains and suggested and commented on the design of the experiments. The manuscript was written by F.C.d.A. and L.-H.T. and commented on by all authors.

COMPETING FINANCIAL INTERESTS

The authors declare no competing financial interests.

Published online at http://www.nature.com/doifinder/10.1038/nn.3141.
Reprints and permissions information is available online at http://www.nature.com/reprints/index.html.

1. Spruston, N. Pyramidal neurons: dendritic structure and synaptic integration. *Nat. Rev. Neurosci.* **9**, 206–221 (2008).
2. Mukaetova-Ladinska, E.B., Arnold, H., Jaros, E., Perry, R. & Perry, E. Depletion of MAP2 expression and laminar cytoarchitectonic changes in dorsolateral prefrontal cortex in adult autistic individuals. *Neuropathol. Appl. Neurobiol.* **30**, 615–623 (2004).
3. Raymond, G.V., Bauman, M.L. & Kemper, T.L. Hippocampus in autism: a Golgi analysis. *Acta Neuropathol.* **91**, 117–119 (1996).
4. Larkman, A.U. Dendritic morphology of pyramidal neurones of the visual cortex of the rat: III. Spine distributions. *J. Comp. Neurol.* **306**, 332–343 (1991).
5. Chen, Z. & Cobb, M.H. Regulation of stress-responsive mitogen-activated protein (MAP) kinase pathways by TAO2. *J. Biol. Chem.* **276**, 16070–16075 (2001).
6. Chen, Z. *et al.* TAO (thousand-and-one amino acid) protein kinases mediate signaling from carbachol to p38 mitogen-activated protein kinase and ternary complex factors. *J. Biol. Chem.* **278**, 22278–22283 (2003).
7. Weiss, L.A. *et al.* Association between microdeletion and microduplication at 16p11.2 and autism. *N. Engl. J. Med.* **358**, 667–675 (2008).
8. McCarthy, S.E. *et al.* Microduplications of 16p11.2 are associated with schizophrenia. *Nat. Genet.* **41**, 1223–1227 (2009).
9. Darnell, J.C. *et al.* FMRP stalls ribosomal translocation on mRNAs linked to synaptic function and autism. *Cell* **146**, 247–261 (2011).
10. Chen, Z., Hutchison, M. & Cobb, M.H. Isolation of the protein kinase TAO2 and identification of its mitogen-activated protein kinase/extracellular signal-regulated kinase kinase binding domain. *J. Biol. Chem.* **274**, 28803–28807 (1999).
11. Moore, T.M. *et al.* PSK, a novel STE20-like kinase derived from prostatic carcinoma that activates the c-Jun N-terminal kinase mitogen-activated protein kinase pathway and regulates actin cytoskeletal organization. *J. Biol. Chem.* **275**, 4311–4322 (2000).
12. Yasuda, S. *et al.* Activity-induced protocadherin arcadlin regulates dendritic spine number by triggering N-cadherin endocytosis via TAO2beta and p38 MAP kinases. *Neuron* **56**, 456–471 (2007).
13. Zihni, C. *et al.* Prostate-derived sterile 20-like kinase 1-alpha induces apoptosis. JNK- and caspase-dependent nuclear localization is a requirement for membrane blebbing. *J. Biol. Chem.* **282**, 6484–6493 (2007).
14. Gu, C. *et al.* Neuropilin-1 conveys semaphorin and VEGF signaling during neural and cardiovascular development. *Dev. Cell* **5**, 45–57 (2003).
15. Tran, T.S. *et al.* Secreted semaphorins control spine distribution and morphogenesis in the postnatal CNS. *Nature* **462**, 1065–1069 (2009).
16. Chen, G. *et al.* Semaphorin-3A guides radial migration of cortical neurons during development. *Nat. Neurosci.* **11**, 36–44 (2008).
17. Fenstermaker, V., Chen, Y., Ghosh, A. & Yuste, R. Regulation of dendritic length and branching by semaphorin 3A. *J. Neurobiol.* **58**, 403–412 (2004).
18. Bradke, F. & Dotti, C.G. The role of local actin instability in axon formation. *Science* **283**, 1931–1934 (1999).
19. King, I. *et al. Drosophila* tao controls mushroom body development and ethanol-stimulated behavior through par-1. *J. Neurosci.* **31**, 1139–1148 (2011).
20. Barnes, A.P., Solecki, D. & Polleux, F. New insights into the molecular mechanisms specifying neuronal polarity *in vivo*. *Curr. Opin. Neurobiol.* **18**, 44–52 (2008).
21. Witte, H. & Bradke, F. The role of the cytoskeleton during neuronal polarization. *Curr. Opin. Neurobiol.* **18**, 479–487 (2008).
22. Arimura, N. & Kaibuchi, K. Neuronal polarity: from extracellular signals to intracellular mechanisms. *Nat. Rev. Neurosci.* **8**, 194–205 (2007).
23. de Anda, F.C., Meletis, K., Ge, X., Rei, D. & Tsai, L.H. Centrosome motility is essential for initial axon formation in the neocortex. *J. Neurosci.* **30**, 10391–10406 (2010).
24. Zhou, T. *et al.* Crystal structure of the TAO2 kinase domain: activation and specificity of a Ste20p MAP3K. *Structure* **12**, 1891–1900 (2004).
25. Romand, S., Wang, Y., Toledo-Rodriguez, M. & Markram, H. Morphological development of thick-tufted layer V pyramidal cells in the rat somatosensory cortex. *Front. Neuroanat.* **5**, 5 (2011).
26. Polleux, F. & Snider, W. Initiating and growing an axon. *Cold Spring Harb. Perspect. Biol.* **2**, a001925 (2010).
27. Huangfu, W.C., Omori, E., Akira, S., Matsumoto, K. & Ninomiya-Tsuji, J. Osmotic stress activates the TAK1-JNK pathway while blocking TAK1-mediated NF-κB activation: TAO2 regulates TAK1 pathways. *J. Biol. Chem.* **281**, 28802–28810 (2006).
28. Ben-Zvi, A. *et al.* Semaphorin 3A and neurotrophins: a balance between apoptosis and survival signaling in embryonic DRG neurons. *J. Neurochem.* **96**, 585–597 (2006).
29. Tararuk, T. *et al.* JNK1 phosphorylation of SCG10 determines microtubule dynamics and axodendritic length. *J. Cell Biol.* **173**, 265–277 (2006).
30. Bjorkblom, B. *et al.* Constitutively active cytoplasmic c-Jun N-terminal kinase 1 is a dominant regulator of dendritic architecture: role of microtubule-associated protein 2 as an effector. *J. Neurosci.* **25**, 6350–6361 (2005).
31. Oliva, A.A. Jr., Atkins, C.M., Copenagle, L. & Banker, G.A. Activated c-Jun N-terminal kinase is required for axon formation. *J. Neurosci.* **26**, 9462–9470 (2006).
32. Barnat, M. *et al.* Distinct roles of c-Jun N-terminal kinase isoforms in neurite initiation and elongation during axonal regeneration. *J. Neurosci.* **30**, 7804–7816 (2010).
33. Rosso, S.B., Sussman, D., Wynshaw-Boris, A. & Salinas, P.C. Wnt signaling through Dishevelled, Rac and JNK regulates dendritic development. *Nat. Neurosci.* **8**, 34–42 (2005).
34. Chang, L., Jones, Y., Ellisman, M.H., Goldstein, L.S. & Karin, M. JNK1 is required for maintenance of neuronal microtubules and controls phosphorylation of microtubule-associated proteins. *Dev. Cell* **4**, 521–533 (2003).
35. Jeanneteau, F., Deinhardt, K., Miyoshi, G., Bennett, A.M. & Chao, M.V. The MAP kinase phosphatase MKP-1 regulates BDNF-induced axon branching. *Nat. Neurosci.* **13**, 1373–1379 (2010).
36. Lei, K. *et al.* The Bax subfamily of Bcl2-related proteins is essential for apoptotic signal transduction by c-Jun NH_2-terminal kinase. *Mol. Cell Biol.* **22**, 4929–4942 (2002).
37. Yamasaki, T. *et al.* Stress-activated protein kinase MKK7 regulates axon elongation in the developing cerebral cortex. *J. Neurosci.* **31**, 16872–16883 (2011).
38. Jan, Y.N. & Jan, L.Y. Branching out: mechanisms of dendritic arborization. *Nat. Rev. Neurosci.* **11**, 316–328 (2010).
39. Baas, P.W., Black, M.M. & Banker, G.A. Changes in microtubule polarity orientation during the development of hippocampal neurons in culture. *J. Cell Biol.* **109**, 3085–3094 (1989).
40. Kwan, A.C., Dombeck, D.A. & Webb, W.W. Polarized microtubule arrays in apical dendrites and axons. *Proc. Natl. Acad. Sci. USA* **105**, 11370–11375 (2008).
41. Horton, A.C. *et al.* Polarized secretory trafficking directs cargo for asymmetric dendrite growth and morphogenesis. *Neuron* **48**, 757–771 (2005).
42. Shelly, M. *et al.* Semaphorin3A regulates neuronal polarization by suppressing axon formation and promoting dendrite growth. *Neuron* **71**, 433–446 (2011).
43. Nishiyama, M. *et al.* Semaphorin 3A induces CaV2.3 channel-dependent conversion of axons to dendrites. *Nat. Cell Biol.* **13**, 676–685 (2011).
44. Polleux, F., Morrow, T. & Ghosh, A. Semaphorin 3A is a chemoattractant for cortical apical dendrites. *Nature* **404**, 567–573 (2000).
45. Geschwind, D.H. & Levitt, P. Autism spectrum disorders: developmental disconnection syndromes. *Curr. Opin. Neurobiol.* **17**, 103–111 (2007).
46. Just, M.A., Cherkassky, V.L., Keller, T.A., Kana, R.K. & Minshew, N.J. Functional and anatomical cortical underconnectivity in autism: evidence from an FMRI study of an executive function task and corpus callosum morphometry. *Cereb. Cortex* **17**, 951–961 (2007).
47. Walsh, C.A., Morrow, E.M. & Rubenstein, J.L. Autism and brain development. *Cell* **135**, 396–400 (2008).
48. Weiss, L.A., Arking, D.E., Daly, M.J. & Chakravarti, A. A genome-wide linkage and association scan reveals novel loci for autism. *Nature* **461**, 802–808 (2009).
49. Pinto, D. *et al.* Functional impact of global rare copy number variation in autism spectrum disorders. *Nature* **466**, 368–372 (2010).
50. Kelleher, R.J. III & Bear, M.F. The autistic neuron: troubled translation? *Cell* **135**, 401–406 (2008).

ONLINE METHODS

shRNA and fluorescent protein constructs. The *Taok2* shRNA sequences used in this study are as follows:

Taok2 shRNA 1 = CGAGAGGACTTGAATAAGAAA;
Taok2 shRNA 2 = GCATCCTAATACCATTCAGTA;
Taok2 shRNA 3 = GTTCCAGGAGACGTGTAAGATCC.

We used primarily *Taok2* shRNA 1 and 2 throughout the experiments. The *Taok2* shRNA 1–resistant construct (pCMV human *TAOK2*) is from imaGenes (Berlin, Germany), clone IRATp970E03140D. The sequence for the *Nrp1* shRNA is AGAGAAGCCAACCATTATA (ref. 16). The shRNAs sequences used in this study were inserted into a pSilencer vector. A pSilencer vector containing a random-sequence hairpin insert was used as a control for the shRNAs. The Venus (pCAGIG) and mCherry (pCAGIG) plasmids were kindly provided by Z. Xie (Boston University). The F-GFP (pCAGIG-GAP 43-GFP) construct was gift from A. Gartner (University of Leuven, Belgium). The Myc-TAOK2 (pCMV rat *Taok2*) was kindly provided by M. H. Cobb (University of Texas Southwestern Medical Center). The Nrp1-mCherry (plasmid 21934) and MKK7-JNK1 (plasmid 19726) are from Addgene (Cambridge, MA).

Lentiviral production. *Production of plentilox3.7 Taok2 shRNA. Taok2* shRNA was cloned into the plentilox 3.7 vector (Addgene plasmid 11795) as previously described[51]. Briefly, complementary 5′ phosphorylated oligonucleotides FC_TAOK2 sh3pllf and FC_TAOK2 sh3pllr with the sequences TGCGAGAG GACTTGAATAAGAAATTCAAGAGATTTCTTATTCAAGTCCTCTCGTT TTTTC and TCGAGAAAAAACGAGAGGACTTGAATAAGAAATCTCTTG AATTTCTTATTCAAGTCCTCTCGCA, respectively, were annealed, digested with XhoI, and ligated into the plentilox 3.7 vector that had been digested with HpaI and XhoI. Proper insertion and orientation of the sequence downstream of the U6 promoter was confirmed using a sequencing primer with the sequence CAGTGCAGGGGAAAGAATAGTAGAC.

Production and titration of virus. Lentiviral particles were made as previously described[51]. Briefly, HEK-293T cells were plated on 10-cm dishes in 10% FBS-DMEM and transfected at 95% confluency with 8 µg plenti 3.7, 6 µg pCMV-R8.9, and 5 µg pCMV-VSV-G per dish. The culture medium was switched to 30% FBS DMEM 12 h after transfection and viral supernatant was collected 48 and 96 h later. Viral supernatant was filtered through a 0.45-µm cellulose acetate vacuum filter (Corning 431155) and concentrated by ultracentrifugation at 25,000*g* for 90 min. Viral pellets were resuspended in Dulbecco's PBS + 0.1% glucose and stored at −80 °C. Viral titers were determined on HEK-293T cells plated at 2×10^5 cells per well in six-well plates, and serial dilutions of 1:200, 1:2,000, and 1:20,000 were used to determine viral titer. After 48 h of viral supernatant application, percentages of infected cells were determined by determining the percentage of fluorescent cells divided by the total number of cells by visual inspection. Four fields of view were counted per well, and three wells were inspected per dilution. Infection was performed with MOI = 10.

Antibodies. The following antibodies were used in these studies: mouse anti-acetylated tubulin (Sigma T7451, immunocytochemistry, 1:1,000), goat anti-TAOK2 (K-16, Santa Cruz Biotechnology, western blot (WB) 1:2,000; immunocytochemistry, 1:100), rabbit anti-pTAOK2 (Ser 181; sc-135712; Santa Cruz Biotechnology; WB, 1:250; immunocytochemistry, 1:100), mouse anti-pJNK1/2 (Cell Signaling Technology 92555, WB 1:250); rabbit anti-pJNK1/2 (Promega V793B, immunocytochemistry, 1:200), mouse anti-pan-JNK (BD Transduction Laboratories 610627; WB, 1:500); rabbit anti-FAK (clone C-20, Santa Cruz Biotechnology sc-558, WB, 1:500); goat anti–rat neuropilin-1 (R&D Systems AF566, WB, 1:500); anti-mCherry (Clontech cat. no. 632543, WB, 1:1,000); anti-RFP (Abcam, ab62341, WB, 1:400); anti-actin (Sigma A5316, clone AC-74, WB, 1:2,000) and anti-GAPDH (WB Santa Cruz Biotechnology sc-32233, 1:500). Nuclei were visualized with Hoechst (Invitrogen) and F-actin with phalloidin (Molecular Probes). Alexa-conjugated secondary antibodies (Jackson ImmunoResearch, 1:1,000) were applied for 1–2 h at 25 °C.

Cell transfection and western blot analysis. HEK-293T and Ht22 cells (ATCC) were grown under standard cell culture conditions and transfected with plasmids using Lipofectamine 2000 according to the manufacturer's protocol (Invitrogen). Proteins from cell lysates were separated on 8% or 12% SDS-polyacrylamide gels at 60m V and transferred to Immobilon-P PVDF membranes (Millipore). Membranes were blocked in TBS-T (50 mM Tris-HCl pH 7.4, 150 mM NaCl, 0.1% Tween-20) with 5% non-fat dry milk for 1 h at room temperature and then incubated with primary antibody for 2 h to overnight at 4 °C. Membranes were washed for 30 min in TBS-T and incubated for 1 h at room temperature with horseradish peroxidase–conjugated secondary antibodies (GE) and then washed for 30 min in TBS-T. Immunoreactivity signals were detected by enhanced chemiluminescence (PerkinElmer).

Immunoprecipitation. *HEK-293T cell lysates.* For transient transfection, HEK-293 cells were cotransfected with equal amounts of overexpression plasmids carrying *myc-Taok2* and *mCherry-Nrp1* cDNA. The total amount of transfected DNA was between 3.5 and 4.0 µg per 35 mm plate. The cells were allowed to express the constructs for 24 h before lysis and analysis. Transfected cells were washed once with ice-cold PBS and immediately lysed in lysis buffer with protease inhibitors. The Bio-Rad assay kit was used to determine protein concentration. For TAOK2 and Nrp1 immunoprecipitation assays, lysates were incubated with protein A–Sepharose conjugated to anti-mCherry overnight at 4 °C. Lysates containing 0.5 mg of protein were used for each condition. The beads were then washed with RIPA buffer twice to remove nonspecific proteins and then washed five times with lysis buffer before boiling in Laemmli sample buffer. Following SDS-PAGE to separate the proteins, blots were incubated with anti-TAOK2.

Cortical brain lysates. Cortices from P0 Swiss Webster mice were dissected and homogenized in 350 µl of sterile-filtered 50 mM Tris-Cl pH 7.4, 120 mM NaCl, 0.5% NP-40 containing proteinase inhibitors (Roche) using a 26G syringe, followed by a 15-min centrifugation at 14,000 r.p.m. at 4 °C and collection of the supernatant. Following a 60-min incubation with 1–2 µg of the corresponding antibodies, 20 µl of protein G–Sepharose (GE Healthcare) was added to the lysates and incubated for 45 min at 4 °C. The bound immune complexes were then collected at 8000 r.p.m. for 3 min followed by one wash each in sterile-filtered 50 mM Tris-Cl, pH 7.4, 500 mM NaCl, 1% NP-40; and sterile-filtered 50 mM Tris-Cl pH 7.4, 120 mM NaCl, 0.5% NP-40. Samples were boiled for 5 min at 95 °C, run on a 10% SDS gel and analyzed with the same primary antibodies used for the immunoprecipitation.

***In utero* electroporation.** The Institutional Animal Care and Use Committee of the Massachusetts Institute of Technology approved all experiments. Pregnant Swiss Webster mice were anesthetized by intraperitoneal injections of ketamine 1% / xylazine 2 mg/ml (0.01 ml/g body weight), the uterine horns were exposed, and plasmids mixed with Fast Green (Sigma) were microinjected into the lateral ventricles of embryos. The shRNA plasmid concentration was two to three times that of mCherry, Venus, or F-GFP. Five current pulses (50 ms pulse, 950 ms interval; 35–36 V) were delivered across the heads of the embryos.

Cortical cultures. Neurons were transfected by *in utero* electroporation at E15 and the transfected cortices were dissected 2 d later. Cortical neurons were isolated in HBSS (Invitrogen) containing papain and DNase at 37 °C (Worthington). Papain was inhibited by the addition of ovomucoid (Worthington). Neurons were plated on poly-D-lysine and laminin pre-coated glass coverslips in Neurobasal / B27 medium (Invitrogen), maintained in culture for 48 h, and then fixed for immunofluorescence analysis. Neurons treated with Sema3A were dissected from brains harvested at E17 and cultured as above. Sema3A (R&D Systems) was applied 48 h later at a final concentration of 2 µg/ml. Neurons infected with lentiviral particles (infected 3 h after plating) were treated with Sema3A for 6 h after 4 d in culture. Cells were either fixed as described for immunofluorescence studies or lysed with cold RIPA buffer supplemented with phosphatase and protease inhibitors (Roche) for western blot analysis.

Immunofluorescence. *Dissociated neurons.* Neurons were fixed with 4% formaldehyde at 37 °C for 2 min followed by fixation for 3 min in methanol at −20 °C. After blocking in goat serum (Zymed), neurons were incubated with the primary antibodies.

Cortical sections. Brains were removed and fixed overnight in 4% formaldehyde and thereafter transferred to 30% sucrose/PBS (4 °C, overnight). Brains were

doi:10.1038/nn.3141

embedded in OCT compound and sectioned in a cryostat. The 20–30 μm cryosections were incubated overnight at 4 °C with the primary antibodies.

Confocal imaging. Images were taken with a Zeiss LSM 510 confocal microscope. *z*-series images were collected with 1-μm steps. To perform 3D reconstructions on stacks of images of transfected cells, only *z* sections in the same focal plane as GFP were used for analysis and for producing figures. 3D reconstructions and *z*-stack analyses were produced using ImageJ software. Brightness and contrast were adjusted.

Quantitative phalloidin fluorescence determination in growth cones. Neurons were cultured for 2DIV after plating and then fixed as described above (see Immunofluorescence). F-actin was visualized by the binding of fluorescently labeled phalloidin. The mean intensity gray value of phalloidin in the growth cone area was measured using ImageJ.

Quantitative immunofluorescence of pTAOK2, pJNK, tubulin and MAP2 in neurites of cultured cortical neurons. Neurons were cultured for 2 DIV and 7 DIV after plating and then fixed as described (see Immunofluorescence). pTAOK2, pJNK, tubulin, and MAP2 were visualized by indirect immunofluorescence. The mean intensity gray value of a line drawn along the neurites was measured using ImageJ.

Sholl analysis. All GFP-positive image stacks from transfected cortical neurons were taken as described (see Confocal imaging). All Sholl analyses use cortices that displayed relatively low transfection efficiencies in order to be able to select and analyze isolated transfected neurons in the cortex. Sholl analysis was performed by drawing concentric circles centered on the cell soma using Adobe Illustrator CS3. The starting radius was 15 μm and the ending radius was 55–100 μm; the interval between consecutive radii was 5 μm. All analyses were performed in a blinded manner.

Statistical analysis. Compiled data are expressed as mean ± s.e.m. We used the two-tailed Student's *t* test and one-way ANOVA, with *post hoc* Tukey or Dunnett tests, for statistical analyses. The *P* values in the Results are from *t* tests unless specified otherwise. $P < 0.05$ was considered statistically significant.

51. Mao, Y. *et al.* Disrupted in schizophrenia 1 regulates neuronal progenitor proliferation via modulation of GSK3beta/beta-catenin signaling. *Cell* **136**, 1017–1031 (2009).

Corrigendum: Autism spectrum disorder susceptibility gene *TAOK2* affects basal dendrite formation in the neocortex

Froylan Calderon de Anda, Ana Lucia Rosario, Omer Durak, Tracy Tran, Johannes Gräff, Konstantinos Meletis, Damien Rei, Takahiro Soda, Ram Madabhushi, David D Ginty, Alex L Kolodkin & Li-Huei Tsai
***Nat. Neurosci.* 15, 1022–1031 (2012); published online 10 June 2012; corrected after print 9 July 2012**

In the version of this article initially published, the scale bar length for Figure 7d was not given. The bar represents 10 µm. The error has been corrected in the HTML and PDF versions of the article.